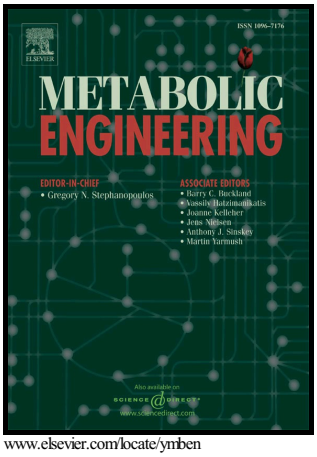


www.elsevier.com/locate/ymben

# Biosensor-assisted transcriptional regulator engineering for Methylobacterium extorquens AM1 to improve mevalonate synthesis by increasing the acetyl-CoA supply

Wei-Fan Liang, Lan-Yu Cui, Jin-Yu Cui, Kai-Wen Yu, Song Yang, Chong Zhang, Xin-Hui Xing

PII: S1096-7176(16)30152-5
DOI: http://dx.doi.org/10.1016/j.ymben.2016.11.010
Reference: YMBEN1186

To appear in: *Metabolic Engineering*

Received date: 2 October 2016
Revised date: 8 November 2016
Accepted date: 28 November 2016

Cite this article as: Wei-Fan Liang, Lan-Yu Cui, Jin-Yu Cui, Kai-Wen Yu, Song Yang, Chong Zhang and Xin-Hui Xing, Biosensor-assisted transcriptiona regulator engineering for Methylobacterium extorquens AM1 to improv mevalonate synthesis by increasing the acetyl-CoA supply, *Metaboli Engineering,* http://dx.doi.org/10.1016/j.ymben.2016.11.010

# Biosensor-assisted transcriptional regulator engineering for Methylobacterium extorquens AM1 to improve mevalonate synthesis by increasing the acetyl-CoA supply

Wei-Fan Liang[a], Lan-Yu Cui[a], Jin-Yu Cui[b], Kai-Wen Yu[c], Song Yang[b], Chong Zhang[a,*], Xin-Hui Xing[a]

[a]Department of Chemical Engineering, Tsinghua University, Beijing 10084, China

[b]School of Life Sciences, Qingdao Agricultural University, Qingdao 266109, China

[c]College of Chemistry and Molecular Engineering, Peking University, Beijing 10084, China

* Corresponding author:

Chong Zhang

E-mail: chongzhang@tsinghua.edu.cn

Telephone: 86-10-62772294

,Fax: 86-10-62787472

Abstract

Acetyl-CoA is not only an important intermediate metabolite for cells but also a significant precursor for production of industrially interesting metabolites. Methylobacterium extorquens AM1, a model strain of methylotrophic cell factories using methanol as carbon source, is of interest because it produces abundant coenzyme A compounds capable of directing to synthesis of different useful compounds from methanol. However, acetyl-CoA always does not efficiently accumulate in M.extorquens AM1, as it is located in the center of three cyclic central metabolic pathways. Here we successfully demonstrated a strategy for sensor-assisted transcriptional regulator engineering (SATRE) to control metabolic flux re-distribution to increase acetyl-CoA flux from methanol for mevalonate production in M.extorquens AM1 with introduction of mevalonate synthesis pathway. A mevalonate biosensor was constructed and we succeeded in isolating a mutated strain (Q49) with a 60% increase in MEV concentration (an acetyl-CoA–derived product) following sensor-based high-throughput screening of a QscR transcriptional regulator library. The mutated QscR-49 regulator (Q8*,T61S,N72Y,E160V) lost an N-terminal α-helix and underwent a change in the secondary structure of the RD-I domain at the C terminus, two regions that are related to its interaction with DNA. $^{13}C$ labeling analysis revealed that acetyl-CoA flux was improvement by 7% and transcriptional analysis revealed that QscR had global effects and that two key points, NADPH generation and fumC overexpression, might contribute to the carbon flux re-distribution. A fed-batch fermentation in a 5-L bioreactor for QscR-49 mutant

yielded a mevalonate concentration of 2.67g/L, which was equivalent to an overall yield of 0.055mol acetyl-CoA/mol methanol, the highest yield among engineered strains of M. extorquens AM1. This work was the first attempt to regulate M. extorquens AM1 on transcriptional level and provided molecular insights into the mechanism of carbon flux regulation.

Key words: Methylobacterium extorquens AM1; QscR regulation; Biosensor; Cyclic pathway; Acetyl-CoA; Mevalonate；

## 1. Introduction

Acetyl-CoA is one of the most important intermediate metabolites in organisms that is widely used as a precursor for production of industrially interesting compounds including terpenoids (e.g., flavors, biofuels and pharmaceuticals), lipids (e.g.,biodiesels and dietary supplements), polyketides and polyhydroxyalkanoates (Pietrocola et al., 2015). The most well-studied acetyl-CoA–mediated strains for bioproductions are Escherichia coli and Saccharomyces cerevisiae, which have been intensively investigated for more than 60 years. However, the use of sugars in these microbial systems as the feedstocks to generate acetyl-CoA has led to some debate about competing uses for human foods and the resulting high costs. It is more and more important to explore alternative carbon sources for production of different useful metabolits via acetyl-CoA synthesis.

Methylobacterium extorquens AM1, an aerobic facultative methylotrophic α-proteobacterium, can use reduced one-carbon compounds such as methanol as its sole carbon and energy source (Chistoserdova et al., 2003), which could make this methylothrophic cell factory (MeCF) economically competitive with the sugar-based ones (Schrader et al., 2009). M. extorquens AM1 could be a potential methanol-based production platform via acetyl-CoA, as it has abundant acetyl-CoA flux within its central metabolic pathways (Alber, 2011). By using acetyl-CoA as a precursor, syhthesis of mevalonate acid (Zhu et al., 2016), α-humulene (Sonntag et al., 2015), 1-butanol (Hu and Lidstrom, 2014) and PHB-co-3HV (Orita et al., 2014) have been

reported. These products, however, always synthesized at very low yields, suggesting that the supply or accumulation of acetyl-CoA was still the bottleneck problem.

Acetyl-CoA is located in the cyclic central metabolic pathways in MeCF-the serine cycle, the citric acid (TCA) cycle and the ethylmalonyl-CoA (EMC) pathway, which are correlated with one another. Improper modification of a single pathway will interrupt the balance of these three correlated central pathways, resulting in growth inhibition or even cell death on the methanol carbon source (Hu and Lidstrom, 2014; Orita et al., 2014; Shen and Wu, 2007). Thus, unlike E. coli or S. cerevisiae, rational push-pull-block strategies to increase precursor supply of acetyl-CoA are, in many cases, invalid for M. extorquensAM1. Global transcription machinery engineering (gTME) (Alper et al., 2006), a non-targeted strategy, has successfully reprogrammed the cellular transcriptome by engineering transcriptional regulators (Klein-Marcuschamer and Stephanopoulos, 2008; Santos et al., 2012). For M. extorquens AM1, QscR, a LysR-type transcriptional regulator that acts as a positive transcriptional regulator for most of the genes involved in the serine cycle (Kalyuzhnaya and Lidstrom, 2005, 2003), could be a potential engineering candidate to redirect the metabolic flux to increase the acetyl-CoA supply for its downstream synthesis of metabolites. However, no attempts have been made to engineer the QscR to date in M. extorquens AM1.

Most examples of gTME have involved tolerance engineering, in which the desired phenotype can be easily screened for by lethal selection (Klein-Marcuschamer and Stephanopoulos, 2008; Tan et al., 2016). Only a few studies focused on the

production of the metabolites such as lycopene (Alper and Stephanopoulos, 2007), avermectin (Zhuo et al., 2010) and L-tyrosine (Santos et al., 2012). Among these, color-based high-throughput screening was most frequently used, which is not suitable for most metabolites without color. In recent years, the use of small-molecule biosensors, which can transform intracellular metabolite concentration into a fluorescent signal, have become a more attractive high-throughput screening method by combining with flowcytometry (Fang et al., 2016; Raman et al., 2014; Tang and Cirino, 2011; Xu et al., 2014). In this study, to redistribute the metabolic flux to increase the acetyl-CoA supply in M. extorquens AM1 from methanol, we tried to use a novel approach that combines the advantages of gTME and small-molecule biosensors: sensor-assisted transcriptional regulator engineering (SATRE),

In this study, mevalonate, a downstream product of acetyl-CoA, was chosen as the target product by introducing mevalonate pathway into M. extorquens AM1. Mevalonate is also the precursor of more than 50,000 terpenoids via the downstream pathway. A mevalonate biosensor was first constructed and characterized in M. extorquens AM1 containing mevalonate synthesis pathway. This biosensor was then used in high throughput screening of the constructed QscR mutant library by combining with fluorescence-activated cell sorting (FACS) to obtain the target mutants with the increased production of mevalonate, i.e., enlargement of acetyl-CoA supply (Fig. 1). By only subsequently overexpressing the mutated QscR-49 (Q8*, T61S, N72Y, E160V), we obtained an engineered M. extorquens AM1 with the highest known level of mevalonate production from methanol (mevalonate

concentration: 2.67 g/L, equivalent yield: 0.055mol acetyl-CoA/mol methanol in a 5-L fermenter).

## 2. Materials and methods

### 2.1. Chemicals, strains, plasmids and media

Mevalonolactone and antibiotics were purchased from Sigma-Aldrich (China) and mevalonolactone was pre-treated according to the literature (Martin et al., 2003). Chemical reagents were purchased from Sinopharm Chemical Reagent Corporation in China. DNA polymerase, restriction enzymes and ligases were purchased from New England Biolabs in China.

Strains and plasmids used in this work are summarized in Table 1. E. coli DH5α (Biomed), which was used for plasmid construction, was grown at 37°C in Luria-Bertani (LB) medium (Bertani, 1951). M. extorquens AM1 was purchased from NCIMB (NCIMB9133). MC minimum medium containing 1% (v/v) methanol was used to cultivate M. extorquens AM1 and its derivative strains (Zhu et al., 2016). Solid medium was prepared by adding 1.5% agar (w/v). Antibiotic was added if necessary. Standard working concentrations of tetracycline, kanamycin, ampicillin and chloramphenicol were 10μg/mL, 50μg/mL, 100μg/mL and 34μg/mL. Cell density was measured by the optical density (OD) at 600 nm ($OD_{600}$). Standard cultivation procedures for M. extorquens AM1 and its derivatives were carried out as follows. Strains were pre-cultivated in 10mL MC medium in a 50-mL flask at 30°C in a rotary shaker at 170rpm until the $OD_{600}$ reached 3-4. Then the seed culture was sub-cultured

in 100mL fresh MC medium ina 500-mL flask with an initial $OD_{600}$ of 0.25 at 30°C in a rotary shaker at 170rpm for 5 days. During this process, the $OD_{600}$ and mevalonate concentration were measured every day. 48 well deep-well plate cuture was the same as above except the culture volume was set as 1.5 mL. The $OD_{600}$and mevalonate concentration were measured at the end of fermentation. All experiments were carried out as biological triplicates.

2.2. DNA manipulations

All primers (Table S1) were purchased from Taihe Biotechnology Co., LTD (Beijing, China). All cloning was carried out as described (Sambrook and Russell, 2001). All constructed plasmids were confirmed by sequencing by Taihe Biotechnology Co., LTD.

2.2.1. Plasmid backbone

The tetracycline resistance gene within the pCM110 plasmid (Marx and Lidstrom, 2001) was replaced with the ampicillin or chloramphenicol resistance gene to generate pCM110A or pCM110C, respectively. Specifically, pCM110 was used as the template for PCR amplification of the plasmid backbone using the primer pairbackbone-F and backbone-R, and pUC19 or pCom10 was used as the template for PCR amplification of the resistance geneusing the primer pair 110A-F and 110A-R or 110C-F and 110C-R, respectively. The resistance gene was assembled with the plasmid backbone via Gibson Assembly (Gibson et al., 2009) to created pCM110A or pCM110C.

2.2.2. Mevalonate biosensor

Sensor-1 fragment was synthesized by GenScript Co., LTD (China) as based on pUC57-sensor (Tang and Cirino, 2011). The construction of pSensor-1, pSensor-2 and pSensor-3 is described in the supplementary material (Fig. S2). pSensor-3 was used as the template for amplification of the $P_{mxaF}$-arac-$P_{BAD}$ fragment and the sfgfp fragment using primer pairs $P_{mxaF}$-F and $P_{BAD}$-R and Sfgfp-F and Sensor-1-R, respectively. These two fragments were assembled with HindIII/KpnI-digested pCM110C to construct pSensor-4.

The integration of Sensor-4 into the M. extorquens AM1 genome required additional subcloning steps. First, pT18 was derived from pK18mobsacB by replacing the gene encoding kanamycin resistance with the gene for tetracycline resistance. pK18mobsacB was used as a template to amplifythe pT18 backboneusing the primer pair K18-F and K18-R, and pCM110 was used as the template to amplify the tetracycline resistance gene using the primer pair Tet-F and Tet-R. The template was digested with DpnI. The pT18 backbone and the tetracycline resistance gene were assembled via Gibson Assembly to create pT18. pT18 was digested with EcoRIand HindIII to linearize the plasmid.Second, theM. extorquens AM1 genome was used as the template to amplify the upstream and downstream fragment of the celABC gene cluster using the primer pairs Cel-up-F and Cel-up-R and Cel-down-F and Cel-down-R, respectively. Third, pSensor-4 was used as the template to amplify the Sensor-4 fragment using the primer pair Sensor-4F and Sensor-4R. Finally, linearized

pT18, the upstream fragment, the Sensor-4 fragment and the downstream fragment were assembled via Gibson Assembly to create pT18-Sensor-4. pT18-Sensor-4 was used to insert Sensor-4 into the celABC site in M. extorquens AM1ΔcelABC by homologous recombination (Marx, 2008) to generate strain S.

2.2.3. Mvt-3 plasmid for mevalonate synthesis

Mvt-3 plasmid (pMvt-3) for mevalonate synthesis from acetyl-CoA was optimized from pARBSU1 (Zhu et al., 2016), which contains the entire mevalonate synthesis pathway. The expression level of the gene encoding HMGR was optimized by RBS engineering (see Table S2). The pARBSU1 was used as the template to amplify the backbone and the optimized HMGR. The backbone was amplified by primer pair Mvt-2F and Mvt-2R, and the HMGR was amplified by the primer pair HMGR-3F and HMGR-3R, which contains the optimized RBS sequence. The template was digested with DpnI.The backbone and the optimized HMGR were assembled via Gibson Assembly to create pMvt-3.

2.2.4. Mevalonate-producing strains

To generate pT18-Mvt-3 to introduce mevalonate synthesis into M. extorquens AM1, the genome of M. extorquens AM1 was used as the template to amplify upstream and downstream fragments of the attTn7site. The upstream fragment was amplified with the primer pair Att-up-F and Att-up-R, and the downstream fragment was amplified with the primer pair Att-down-F and Att-down-R. pMvt-3 was used as

the template to amplify Mvt-3 mevalonate synthesis pathway containing kanamycin resistance using the primer pair Mvt-3F and Mvt-3R. Linearized pT18 (as described above), the upstream fragment, the Mvt-3 fragment and the downstream fragmentwere assembled via Gibson Assembly to create pT18-Mvt-3. pT18-Mvt-3 was used to insert the Mvt-3 pathway into the attTn7 site of the M. extorquens AM1 strain S by homologous recombination to generate strain MS.

pMvt-3 was also electroporated into strain S to create strain MS-2, and pARBSU1 was electroporated into strain MS to create strain MS-3.

2.2.5. Evaluation of the QscR regulator

To evaluate the QscR regulator, we attempted to knock out endogenous qscr. The genome of M. extorquens AM1 was used as the template to amplify the upstream and downstream fragments of qscr using the primer pairsk-qscr-up-F and k-qscr-up-R and k-qscr-down-F and k-qscr-down-R, respectively. Linearized pT18 (as described above), the upstream fragment of qscr andthe downstream fragment of qscr were assembled via Gibson Assembly to create pT18-qscr. pT18-qscr was used to knockout endogenous qscr by homologous recombination.

To overexpress qscr, pCM110A was used as the template to amplify the backbone using the primer pair CM110-F and CM110-R. The genome of M. extorquens AM1 was used as the template to amplify qscr using the primer pair Qscr-F and Qscr-R. The amplified plasmid backbone and qscr were assembled via

Gibson Assembly to create pCM110A-qscr. pCM110A-qscr was electroporated into the MS strain.

To overexpress ftfl, the genome of M. extorquens AM1 was used as the template to amplify ftflwith the primer pair Ftfl-F and Ftfl-R. The pCM110A backbone (as described above) and the amplified ftfl were assembled via Gibson Assembly to create pCM110A-ftfl. pCM110A-ftfl was electroporated into the MS strain.

The resulting strains were cultured as described in section 2.1.

2.3. Generation and screening of QscR mutant library

A QscR mutant library on the pCM110C backbone was created by error-prone PCR with primer pair Qscr-ep-F and Qscr-ep-R to generate low mutation frequencies (2–6 mutations/kb). To replace the $P_{mxaF}$ promoter in pCM110C with the native $P_{qscr}$ promoter to drive the expression of the mutated qscr genes in M. extorquens AM1, the $P_{qscr}$ promoter fragment was first amplified with primer pair Pqscr-F and Pqscr-R. Then pCM110C was digested with HindIII and KpnI to remove the $P_{mxaF}$ promoter and multicloning site. The plasmid backbone, $P_{qscr}$ promoter fragment and mutated qscr fragments were assembled via Gibson Assembly to generate the pQscR mutant library. The pQscR library was electroporated into strain MS to generate a QscR mutant strain library, and the resulting strain library was grown on MC plates containing chloramphenicol antibiotic. A total of 20 plates were carried out and there were at least 2000 colonies on each plate. After 5 days, colonies were transfered into 10 mL fresh liquid MC medium in a 50-mL flask and subcultured for 5 days. Single

cells with the highest fluorescence (indicating the highest mevalonate levels) were then isolated by FACS (see section 2.5). Single-cell subculture and fermentation were carried out in 48-well deep-well plates.

To reconstruct pQ49, the mutant Q49 strain (isolated from the QscR strain library) was used as the template for colony PCR to amplify the mutated qscr-49 using primer pair Qscr-ep-F and Qscr-ep-R and to amplify the plasmid backbone using primer pair CM110-F and Pqscr-R. The mutated qscr-49fragment and backbone were assembled via Gibson Assembly to create pQ49. pQ50 was similar to pQ49, except the mutated qscr-49 was replaced with qscr-50 amplified using the primer pair Q50-F and Qscr-ep-R.

2.4. Extraction of intracellular mevalonate

The extraction of intracellular mevalonate was carried out as described (Yang et al., 2013), with some modifications. Cells were cultured in 100mL MC medium in a 500-mL flask, and $10^{10}$ cells were harvested every 24 hrwith a filtration device. Cells on the filtration membrane were washed twice with deionized water, and the membrane was transferred to a 50-mL tubfe in liquid nitrogen for quenching. Boiling water (10 mL) was added to the tube, and the tube was incubated in a water bath at 100°C for 12 min. The tube was centrifuged at 10,000 ×g at 4°C for 10 min, and an 8-mL portion of the supernatant was then transferred to a new 50-mL tube. The supernatant was dried in a freeze dryer (FDU-1100, EYELA), and the dried sample was redissolved in 1mL of deionized water. The sample was then centrifuged at

10,000×g for 2 min at room temperature to remove any debris. The supernatant was used to analyze intracellular mevalonate as described below.

2.5. Measurement of mevalonate, methanol and fluorescence

Mevalonate and methanol were detected as described (Zhu et al., 2016). Briefly, fermentation broth was centrifugedat 10,000×g for 2min at room temperature, and the supernatant was used to analyze the methanol concentration by gas chromatography. For mevalonate detection, the supernatant was adjusted to pH $\leq 2$ with 20%(v/v) sulfuric acid and then was incubated in a waterbath at 45°C for 1 hr and extracted with two volumes of ethyl acetate. The organiclayer was used to analyze the mevalonate concentration by gas chromatography.

To measure fluorescence, cell cultures were diluted to an $OD_{600}$ of 0.2–0.8 with PBS buffer, 200 μL cultures were added into 96 well plate and fluorescence was measured with an Infinite M200pro Tecan Fluorescence Reader (excitation wavelength, 485 nm; emission wavelength, 535 nm). Fluorescence was normalized based on the $OD_{600}$ value of the culture. For flow cytometry, cell cultures were diluted to an $OD_{600}$ of 0.1 with PBS buffer, and fluorescence was measured with a FACS Aria flow cytometer (BD Biosciences). Excitation wavelength was 485 nm and emission wavelength was 535 nm. Data were processed using BDFACSDiva software (BD Bioscience).

2.6. $^{13}C$ labeling analysis of acetyl-CoA

$^{13}C$ labeling analysis was performed by the protocol reported before (Yang et al., 2013). $^{13}C$-labeled methanol was purchased from Sigma (St. Louis, MO, USA). Cells were grown in MC medium with $^{12}C$ methanol as the carbon source. In the middle of the exponential phase ($OD_{600}$ = 2.0±0.05), 15 mL of the culture were extracted and rapidly passed through the membrane filter (0.22 μm, 47 mm, Sartorius) using a pipette. The filter was immediately removed and placed on an agar plate of MC medium with $^{12}C$ methanol for 30 min in 30℃, then transferred to another agar plate with the same concentration of $^{13}C$-labeled methanol. At 20 min, the filter was immediately transferred to a 50-mL tube with liquid nitrogen for quenching. The sample was stored in a -80°C freezer until it was ready for subsequent extractions.

The extraction method for in vivo metabolites was modified based on a previous study (Yang et al., 2013). Briefly, 10 mL of boiled water was added to the tube containing the sample and incubated in a water bath at 100 °C for 10 min. The sample was centrifuged at 5000×g at 4 °C for 10 min to remove cell debris. The supernatant was dried in a freeze dryer (FDU-1100, EYELA). The dried sample was dissolved in 1.5 mL of water and centrifuged at 13,000×g at 4 °C for 10 min to remove debris. The supernatant was dried again in the freeze dryer.

The sample was separated on a ZIC-HILIC column (150×4.6 mm, 3 μm, 100 Å pore size; EMD Merck, Billerica, MA, USA) and detected by Agilent LC-QQQ-MS system (Agilent 1290 Infinity-6460). For the metabolites detected in the positive and negative ESI mode, the mobile phase A was 10% (v/v) buffer in water and mobile phase B was 10% (v/v) buffer in acetonitrile. The buffer consisted of 200 mM formic

acid adjusted to pH 4.0 with ammonium hydroxide solution. The linear gradient was as follows: 0–4 min, 100 % B; 4–15 min, 100–81 % B; 15–21 min, 81–70 % B; 21–26 min, 70–40 % B; 26–27 min, 40–100 % B; and 27–39 min, 100 % B. The total run time was 39 min at 0.2 mL/min. The injection volume was 10 μL. The LC-MS/MS experiments were conducted as described previously (Yang et al., 2013). The dwell time for each MRM (multiple reaction monitoring) transition was 25s. All of the peaks were integrated using the Qualitative Analysis B.06.00 software. The $^{13}C$ incorporation of a metabolite with N carbon atoms was calculated by normalizing to its total carbon number according to the previous protocol (Fang et al., 2015).

2.7. Transcriptional analysis

Cells were grown in MC medium to an $OD_{600}$ of ~3.0 (exponential phase). A 2-mL aliquot of the cell culture was centrifuged at 4,500×g for 2 min at room temperature. After removal of the supernatant, the cell pellet was dealt with liquid nitrogen, and then RNA was extracted using the QIAGEN RNeasy Mini kit. RNA sequencing was carried out by Annoroad Genomics Co., LTD (China). Data were processed using Rockhopper software (McClure et al., 2013). Triplicate samples were used for transcriptional analysis.

2.8. Fed-batch fermentation

A 5-L stirred tank bioreactor (Applikon, Delft, TheNetherlands) was used for fermentation with a working volume of 3L. MO medium (Zhu et al., 2016) was used

for fermentation. The seedling culture for the fermentation was as described above (section 2.1). The bioreactor was operated at 30°C with shaking at 500 rpm. The dissolved oxygen concentration was maintained at 35± 5% using compressed air. The pH of the bioreactor was maintained at 6.8 ±0.05 using 10%(v/v) ammonia in water. The methanol concentration was detected off-line every 12hr, and methanol was supplemented manually to maintain a 1%(v/v) concentration.

## 3. Results

### 3.1. Construction and characterization of the mevalonate biosensor

A biosensor for intracellular mevalonate was previously constructed in E. coli by engineering the regulatory protein AraC in the arabinose operon. The mutated AraC-mev (T24L, H80L, Y82L, H93R) responds to a change in the intracellular mevalonate concentration across a 3.8-fold dynamic range in E. coli. (Tang and Cirino, 2011). However, this mevalonate sensor did not function in M. extorquens AM1 (see Fig.S5), as the organisms tightly control their regulatory systems and biosensors based on these mechanisms are often limited in their ability to function in non-native hosts (Mahr and Frunzke, 2016). For this reason, we engineered this biosensor suitable for M. extorquens AM1.

As shown in Fig. 2A, AraC-mev blocks the $P_{BAD}$ promoter in the absence of mevalonate and prevents the transcription of reportor gene sfgfp (Pédelacq et al., 2006). In the presence of mevalonate, mevalonate-bound AraC-mev binds to the$P_{BAD}$ promoter and stimulates transcription of the $P_{BAD}$ promoter via direct interactions with

RNA polymerase (Zhang et al., 1996), and consequently results in the expression of sfGFP. Therefore, the concentration of AraC-mev was the key for transcriptional regulation of the mevalonate biosensor (Fig. S1). We thus first tried to change the promoter, terminator and RBS in the AraC-mev expression cassette to precisely control the expression of AraC-mev (Figs. S2B–D) and then deleted the RBS in the sfGFP expression cassette to weaken the leakage of fluorescent protein expression (Fig. S2E). Finally, the engineered mevalonate biosensor, named Sensor-4, was inserted into the celABC site of the M. extorquens AM1 chromosome by homologous recombination. M. extorquens AM1 with the Sensor-4 integration was named the strain S.

To evaluate the performance of this sensor, strains that generated various concentrations of mevalonate were constructed. The mevalonate-producing plasmid pMvt-3, which was derived from the mevalonate pathway in pARBSU1 (Zhu et al., 2016) and the HMGR was RBS-optimized, was inserted into the genome site attTn7 (Choi et al., 2006) of strain S by homologous recombination with the help of pT18-Mvt-3 to generate strain MS. In addition, pMvt-3 was also electroporated into strain S to create strain MS-2, and pARBSU1 was electroporated into strain MS to create strain MS-3. The extracellular mevalonate concentration and fluorescence intensity of these three strains and of the parental strain S were analyzed. The mevalonate biosensor had a good linear relationship within a range of 0–1.7 mM extracellular mevalonate (Fig. 2B). We also found a positive correlation between extracellular mevalonate and intracellular mevalonate across this same range (Fig.2C).

Thus the fluorescence output of GFP by the biosensor was positively correlated with the intracellular mevalonate concentration.

3.2. Screening for high mevalonate producers

We first confirmed the function of the QscR regulator by changing its expression level (i.e., by deleting genomic qscR or overexpressing qscR) or changing the concentration of its co-inducer (formyl-$H_4F$) by overexpressing ftfl (Kalyuzhnaya and Lidstrom, 2005). As shown in Table S3, there was no difference in the growth of these three resulting strains relative to the parental strain MS, but these changes did strongly influence mevalonate productivity, which indicated that the QscR regulatorcan change carbon flux significantly.

A library of mutated QscR fragments was constructed by error-prone PCR to generate a low frequency of mutations (2-6 mutation/kb) in QscR. The library was then ligated under the control of the native $P_{qscr}$ promoter to generate the pQscR library. MS cells were electroporated with the pQscR library and MS/pQscRs were then cultured for 5 days before FACS sorting. Flow cytometry was used to isolate the cells with high fluorescence. Forty-nine cells with high fluorescence were sorted from the original 2 million cells and were cultured individually in 48-well deep-well plates. Five of these constructed strains had higher mevalonate levels than the control strain MS/pCM110C, indicating a positive rate of 10.2% to the 49 sorted strains (Fig. 3) and 0.00025% to the library. The highest mevalonate-producing strain was MS-QscR-49 (Q49), which had a 60% increase in mevalonate level as compared with control strain.

We further compared the performance of Q49 and control strain by culturing both strains in shake flasks (Fig.4). The growth curve of Q49 was nearly the same as that of control strain. In terms of mevalonate production, however, Q49 showed a more rapid and higher production than control strain. The mevalonate concentration after 5 days in culture was 88 ± 1 mg/L for Q49, which was about 60% higher than that for control strain MS/pCM110C.

3.3. Sequence analysis of the mutant Q49

The fragment of qscr from strain Q49, which encodes the mutated QscR-49, was sequenced. As shown in Fig. 5, there were four mutations (Q8*,T61S,N72Y,E160V) in QscR-49. Because of the introduced stop codon at Q8, the real functional QscR-49 is most likely translated from the second start codon at nucleotide 61. To confirm this hypothesis, the qscr-50 fragment was amplified from the second start codon at nucleotide 61 to generated pQ50. pQ50 had a similar effect on mevalonate production as pQ49 (data not shown), indicating that real effective QscR-49 was most likely translated from nucleotide 61 and the corresponding protein was QscR-50 (T41S,N52Y,E140V). The missing 20 amino acids consisted of part of the DNA-binding domain, and the C-terminal mutated site was located in the RD-I region, which was also related to DNA recognition (Maddocks and Oyston, 2008). The first and second mutated sites of QscR-50 are located in the coiled-coil linker, which connects the N-terminal domain and C-terminal domain (Maddocks and Oyston, 2008).

This was also confirmed by a three-dimensional structure simulation using I-TASSER on-line software (Yang et al., 2015) (Fig.S3). Compared with the original QscR, QscR-50 lost the first α-helix in the N-terminal region, which is located in the DNA-binding domain of wild-type QscR and underwent a change in its secondary structure in the RD-I region. There are three α-helices in the DNA-binding domains of LysR-type regulators in general (Aravind et al., 2005). The second and the third α-helices recognize DNA sequences and the third α-helix interacts with DNA; however, the function of the first α-helix is unknown, although it may participate in DNA recognition (Otting et al., 1990). Thus the improvement in mevalonate production might be due to the structural changes in these two regions, both of which could interact with DNA.

3.4. Fermentation of strain Q49 in a 5-L bioreactor

To evaluate the fermentation performance of the strain Q49, a 5-L fermenter was run by fed-batch fermentation using MO medium (Zhu et al., 2016). The initial methanol concentration was set to 1%(v/v), and methanol was analyzed and supplemented every 12hr to maintain the concentration. Cell growth increased to an $OD_{600}$ of 23.3 within 400hr and mevalonate production was associated with cell growth (Fig. 6). The mevalonate concentration was 2.67 g/L at the end of fermentation, which was equivalent to an overall yield of 0.085 g mevalonate/g methanol and a volumetric productivity of 6.6 mg/L/hr. This would provide at least

the equivalent of 0.055mol acetyl-CoA/mol methanol and it is the highest yield for engineered M. extorquens AM1 to date.

The level of mevalonate produced by strain Q49 was almost the same as that produced by the AM1-ARBSU1 strain constructed previously in our lab (Zhu et al., 2016) for 300 hr fermentation, but the yield achieved by the Q49 strain showed a 2.8-fold increase. There are two differences between the strains of AM1-ARBSU1 and Q49: (1) the mevalonate synthesis pathway is retained on a non-integrated plasmid (about five copies per cell) in AM1-ARBSU1, whereas the pathway is present as a single integrated copy in genome in Q49 and (2) this pathway undergoes QscR regulation in strain Q49. This result indicated that QscR regulation could alter the carbon flux re-distribution and lead to improved production in a single-copy strain as compared with a multi-copy strain without QscR regulation.

3.5. Acetyl-CoA flux analysis and transcriptional analysis of strain Q49

To elucidate the biochemical significance of QscR regulation, Acetyl-CoA flux analysis by $^{13}C$ labeling analysis and transcriptional analysis were used to examine the differences between the control strain MS/pCM110C and the QscR-regulated strain Q49. As shown in Fig. 7, acetyl-CoA flux of Q49 was about 7% higher than that of control strain and this maybe the direct reason for mevalonate improvement in strain Q49. Transcriptional analysis was carried out to look insight into molecular mechanism of carbon flux re-distributiion of Q49.

The Q49 strain had an obviously different pattern of global transcription as compared with MS/pCM110C (Fig. S4). For this analysis, 5012 genes were compared between the two strains and 82 genes exhibited significantly different transcription level (>2-fold, q<0.01).

Of these differentially transcribed genes, most had an unknown function based on KEGG, GO term (BP, CC, MF) and Pfam domain database searches. There were, however, 17 differentially transcribed genes with known functions, and among these several could be classified into three groups: gluconeogenesis, response regulators and transcription and translation processes (see Table S4). Gluconeogenesis-related genes included cbbF and gpmA showed significant up-regulation in Q49 (2-and 3-fold, respectively; q <0.01). The genes that function as a response regulator, such as fixJ, mucR, MexAM1_META1p1157 and MexAM1_META1p0610, which belong to the LuxR, MucR, Crp/Fnr and MarR family of transcriptional regulators, respectively, showed significant down-regulation (2.6- to 4.5-fold, q <0.01). The genes MexAM1_META1ptRNA15 and MexAM1_META1p3777, which are involved in transcription and translation process, also showed a 2.3- and 3.9-fold decrease, respectively. In addition, fumC, which functions in the central cyclic metabolic pathways, had a 2.2-fold increase (q <0.01).

Although the transcription of many genes was significantly affected in the Q49 strain, specific patterns within central metabolic pathways might provide a possible explanation for the carbon re-distribution in this strain. As shown in Table S4, gluconeogenesis and the pentose phosphate pathway were up-regulated, leading

carbon flux into reducing power generation pathway. Transcription of fumC, which is shared by the EMC cycle and the TCA cycle, was increased by 2.2-fold, which might change the carbon flux of the central cyclic metabolic pathways. Other central metabolic pathways and the mevalonate synthesis pathway were unchanged. Taken together, as shown in Fig. 7, our results indicated that up-regulation of fumC transcription might contribute to carbon re-distribution and guide carbon flux into mevalonate synthesis from acetyl-CoA, and up-regulation of gluconeogenesis and the pentose phosphate pathway might increase NADPH generation, which would satisfy the need for NADPH consumption by the heterologous mevalonate synthesis pathway.

## 4. Discussion

M. extorquens AM1 was first isolated in 1960 from soil (Peel D, 1961) and has long been used as a useful MeCF to synthesize single cell protein (Senior and Windass, 1980), amino acids (Sirirote P, Yamane T, 1986) and polyhydroxybutyrate (Bourque D, PomerleauY, 1995). In recent years, characterization of its genome sequence (Vuilleumier et al., 2009) and metabolic network (Peyraud et al., 2011), along with the development of a set of genetic tools and omics data (Ochsner et al., 2014) for M. extorquens AM1 have allowed researchers to develop this methanol-based MeCF with different phenotypes. However, the complexity of the cyclic central metabolic pathways makes it difficult to accumulate acetyl-CoA in M. extorquens AM1. Here we used a SATRE strategy to control metabolic flux

re-distribution and successfully drove the carbon flux into acetyl-CoA toward mevalonate synthesis. As a result, we were able to identify a qscr mutant capable of increasing mevalonate production from acetyl-CoA. This strategy provides not only a method for modifying metabolic flux but also an opportunity for understanding the key regulatory mechanism of carbon flux re-distribution in M. extorquens AM1 for bioproduction.

The LysR-type transcriptional regulators are the most abundant transcriptional regulators in bacteria, and they have similar functions across diverse bacterial species including roles in metabolism, oxygen stress, motility, quorum sensing and so on (Maddocks and Oyston, 2008). QscR, a LysR-type transcriptional regulator, is a regulator of the serine cycle in methylotrophic bacteria and is essential for the growth on methanol. As expected, the Q49 strain, which contains both mutated QscR-49 and endogenous QscR, shows a remarkable effect on carbon flux re-distribution in cyclic pathways of M. extorquens AM1 and no effect on its growth. Therefore, the QscR transcriptional regulator is a notable factor in the regulation of metabolic flux for M. extorquens AM1. Protein structure modeling of QscR-49 showed that two mutations in the linker region have no impact on the secondary structure. However, two mutations in the DBD region and RD-I region, both of which are related to DNA recognition, alter the secondary structure and are likely to change the transcription of related genes. We then knocked out the endogenous qscr in both the Q49 strain and MS strain, but we were unable to isolate strains capable of producing higher mevalonate titer in a second round of screening (data not shown). These results

suggested that the endogenous QscR is crucial for the metabolism on methanol and that both endogenous QscR and mutated QscR-49 contribute to mevalonate synthesis by acetyl-CoA regulation. We also tried to use the common $P_{mxaF}$ promoter in methylotrophes to drive the transcription of the QscR library; however, no positive mutated strains were screened out (data not shown). Overexpressing the QscR led to reduced mevalonate levels (Table S3), demonstrating that endogenous QscR acts as an autorepressor to control gene expression (Kalyuzhnaya and Lidstrom, 2003). In this respect, the $P_{qscr}$ promoter is a substantial contributor to QscR regulation.

Screening method is the limited step for studying the QscR regulation in gTME by the irrational design. The well used screening method for gTME is tolerance, color screening or 96-well plate screening, which are not suitable for most metabolites. Intracellular biosensor-based high throughput screening method has the highest efficiency (2000 cells/second) and feasibility compared with 96-well plate screening (on the order of hundreds of cells per screening) and color screening (1000 cells per plate). More and more biosensors specific for small molecular metabolites have been developed for E. coli or S. cerevisiae. However, no biosensors have been developed for the intracellular metabolites of M. extorquens AM1 up to now and most functional elements from the model strains reported so far can not work directly in M. extorquens AM1 because of the cross-species. Mevalonate biosensor, originally developed for E. coli, was successfully engineered for sensing the intracellular mevalonate in M. extorquens AM1 in this work by three steps modification and a high mevalonate producing strain Q49 with mutated QscR regulator was generated by this

engineered mevalonate biosensor using FACS. Researchers can also use our QscR library to improve other metabolites production as long as a corresponding high-throughput screening method is established.

In the 5-L bioreactor fermentation, the Q49 strain showed at least a 2.8-fold improvement in mevalonate yield as compared with the mevalonate-producing strain without QscR regulation (AM1-ARBSU1 strain). This notable increase in the performance of Q49 was achieved by expressing only a mutated QscR regulator, indicating that the QscR regulator is a powerful tool for regulating the metabolic flux in M. extorquens AM1. In another reported example of fed-batch cultivation, α-humulene production by CM502_pFS62b, an engineered strain of M. extorquens AM1, showed a yield of 0.031g α-humulene/g methanol (approximately equivalent to 0.044 mol acetyl-CoA/mol methanol) (Sonntag et al., 2015). The equivalent yield in terms of acetyl-CoA by strain Q49 was 0.055 mol acetyl-CoA /mol methanol, 25% higher than that of CM502_pFS62b, indicating that oeverepression of the mutated QscR regulator could precisely and efficiently enhance the acetyl-CoA accumulation in cyclic pathways in M. extorquens AM1.

$^{13}C$ labeling analysis to compare strain Q49 and control strain revealed that acetyl-CoA flux was increased by 7%. A transcriptional analysis revealed the diverse significant changes in the transcription of genes including those related to an environmental response and gluconeogenesis. In particular, four response regulators consisting of members of the LuxR, MucR, Crp/Fnr and MarR families of transcriptional regulators were down-regulated. The functions of these regulators

might presumably pertain to the redox state, oxidative stress, quorum sensing, the secretion system, organic solvent tolerance and temperature sensing (Nasser and Reverchon, 2007; Saridakis et al., 2008; Spiro, 1994). Although we do not know the direct relationship between higher mevalonate levels and changes in these regulators, we assumed that these regulators would all provide some benefits by allowing the cells to adapt to a better physiological state after the pathway engineering. These regulators need to be further investigated.

Pathway analysis using the transcription data in strain Q49 further revealed two key points for the metabolic flux re-distribution. The first key point is the NADPH generation. Cells grown on methanol are limited by reducing equivalents (NADH or NADPH) (Guo and Lidstrom, 2006), and the introduction of a heterologous mevalonate synthesis pathway, which consumes NADPH, will enhance this effect. The genes involved in the gluconeogenesis and the pentose phosphate pathway were up-regulated in Q49, suggesting that the carbon flux was shifted to generate NADPH to supplement the NADPH consumption by the mevalonate pathway. It is also possible that NADPH (or $NADP^+$) will affect the binding activity of (mutated) QscR (Kalyuzhnaya and Lidstrom, 2003) and change the regulation of metabolic network, leading to acetyl-CoA accumulation. The second key point is the overexpression of fumC. The mechanism of accumulating mevalonate by overexpression of fumC is still unclear, although it does function in the cyclic pathways. The reaction catalyzed by FumC is shared by the TCA cycle and EMC cycle, and the product of this reaction,

malate, pertains to these three cyclic central pathways. As this reaction is linked to the three cyclic pathways, it might contribute to acetyl-CoA accumulation.

In conclusion, this study demonstrated a SATRE strategy for controlling metabolic flux re-distribution of cyclic pathways in M. extorquens AM1. The QscR transcriptional regulator is precise and efficient in driving metabolic flux into mevalonate via acetyl-CoA by four points mutations. This established mevalonate (acetyl-CoA)-producing platform by the biosensor-based transcriptional regulation can be applied not only to the synthesis of mevalonate-deriven bioproducts but also to the production of other value-added compounds based on acetyl-CoA by replacing the mevalonate synthesis pathway with pathways of other metabolic products.

ACKNOWLEDGMENTS

We thank Dr. Marina G. Kalyuzhnaya from San Diego State University for communicating about the QscR regulator. We thank Dr. Tong Zhao from Flow Cytometry Facility, Institute of Microbiology, Chinese Academy of Science, for assistance with flow cytometry and FACS. This work was supported by the National Natural Science Foundation of China (NSFC 21376137) and Tsinghua University Initiative Scientific Research Program (20131089238).

References

Alber, B.E., 2011. Biotechnological potential of the ethylmalonyl-CoA pathway. Appl. Microbiol. Biotechnol. 89, 17–25. doi:10.1007/s00253-010-2873-z

Alper, H., Moxley, J., Nevoigt, E., Fink, G.R., Stephanopoulos, G., 2006. Engineering Yeast Transcription Machinery for Improved Ethanol Tolerance and Production. Science (80-. ). 314, 1565–1568. doi:10.1126/science.1131969

Alper, H., Stephanopoulos, G., 2007. Global transcription machinery engineering: A new approach for improving cellular phenotype. Metab. Eng. 9, 258–267. doi:10.1016/j.ymben.2006.12.002

Aravind, L., Anantharaman, V., Balaji, S., Babu, M.M., Iyer, L.M., 2005. The many faces of the helix-turn-helix domain: Transcription regulation and beyond. FEMS Microbiol. Rev. 29, 231–262. doi:10.1016/j.femsre.2004.12.008

Bertani, G., 1951. Studies on lysogenesis. I. The mode of phage liberation by lysogenic Escherichia coli. J. Bacteriol. 62, 293–300. doi:citeulike-article-id:149214

Bourque D, PomerleauY, G., 1995. High-celldensity production of poly-b-hydroxybutyrate (PHB) from methanol by methylobacterium extorquens: production of high-molecular-mass PHB. Appl Microbiol Biotechnol 44, 197–204.

Chistoserdova, L., Chen, S., Lapidus, A., Lidstrom, M.E., Chen, S., 2003. Methylotrophy in Methylobacterium extorquens AM1 from a Genomic Point of View. J. Bacteriol. 185, 2980–2987. doi:10.1128/JB.185.10.2980

Choi, Y.J., Bourque, D., Morel, L., Groleau, D., Míguez, C.B., Mı, C.B., 2006. Multicopy Integration and Expression of Heterologous Genes in

Methylobacterium extorquens ATCC 55366. Appl. Environ. Microbiol. 72, 753–759. doi:10.1128/AEM.72.1.753

Fang, M.-Y., Zhang, C., Yang, S., Cui, J.-Y., Jiang, P.-X., Lou, K., Wachi, M., Xing, X.-H., 2015. High crude violacein production from glucose by Escherichia coli engineered with interactive control of tryptophan pathway and violacein biosynthetic pathway. Microb. Cell Fact. 14, 8. doi:10.1186/s12934-015-0192-x

Fang, M., Wang, T., Zhang, C., Bai, J., Zheng, X., Zhao, X., Lou, C., Xing, X.H., 2016. Intermediate-sensor assisted push-pull strategy and its application in heterologous deoxyviolacein production in Escherichia coli. Metab. Eng. 33, 41–51. doi:10.1016/j.ymben.2015.10.006

Gibson, D.G., Young, L., Chuang, R.-Y., Venter, J.C., Hutchison, C. a, Smith, H.O., 2009. Enzymatic assembly of DNA molecules up to several hundred kilobases. Nat. Methods 6, 343–5. doi:10.1038/nmeth.1318

Guo, X., Lidstrom, M.E., 2006. Physiological analysis of Methylobacterium extorquens AM1 grown in continuous and batch cultures. Arch. Microbiol. 186, 139–149. doi:10.1007/s00203-006-0131-7

Hu, B., Lidstrom, M.E., 2014. Metabolic engineering of Methylobacterium extorquens AM1 for 1-butanol production. Biotechnol. Biofuels 7, 156–165. doi:10.1186/s13068-014-0156-0

Kalyuzhnaya, M.G., Lidstrom, M.E., 2005. QscR-Mediated Transcriptional Activation of Serine Cycle Genes in Methylobacterium extorquens AM1. J. Bacteriol. 187, 7511–7517. doi:10.1128/JB.187.21.7511

Kalyuzhnaya, M.G., Lidstrom, M.E., 2003. QscR, a LysR-Type Transcriptional Regulator and CbbR Homolog, Is Involved in Regulation of the Serine Cycle Genes in Methylobacterium extorquens AM1. J. Bacteriol. 185, 1229–1235. doi:10.1128/JB.185.4.1229-1235.2003

Klein-Marcuschamer, D., Stephanopoulos, G., 2008. Assessing the potential of mutational strategies to elicit new phenotypes in industrial strains. Proc. Natl. Acad. Sci. U. S. A. 105, 2319–2324. doi:10.1073/pnas.0712177105

Maddocks, S.E., Oyston, P.C.F., 2008. Structure and function of the LysR-type transcriptional regulator (LTTR) family proteins. Microbiology 154, 3609–3623. doi:10.1099/mic.0.2008/022772-0

Mahr, R., Frunzke, J., 2016. Transcription factor-based biosensors in biotechnology: current state and future prospects. Appl. Microbiol. Biotechnol. 100, 79–90. doi:10.1007/s00253-015-7090-3

Martin, V.J.J., Pitera, D.J., Withers, S.T., Newman, J.D., Keasling, J.D., 2003. Engineering a mevalonate pathway in Escherichia coli for production of terpenoids. Nat. Biotechnol. 21, 796–802. doi:10.1038/nbt833

Marx, C.J., 2008. Development of a broad-host-range sacB-based vector for unmarked allelic exchange. BMC Res. Notes 1, 1. doi:10.1186/1756-0500-1-1

Marx, C.J., Lidstrom, M.E., 2001. Development of improved versatile broad-host-range vectors for use in methylotrophs and other gram-negative bacteria. Microbiology 147, 2065–2075. doi:10.1099/00221287-147-8-2065

Nasser, W., Reverchon, S., 2007. New insights into the regulatory mechanisms of the LuxR family of quorum sensing regulators. Anal. Bioanal. Chem. 387, 381–390. doi:10.1007/s00216-006-0702-0

Ochsner, A.M., Sonntag, F., Buchhaupt, M., Schrader, J., Vorholt, J.A., 2014. Methylobacterium extorquens: methylotrophy and biotechnological applications. Appl. Microbiol. Biotechnol. doi:10.1007/s00253-014-6240-3

Orita, I., Nishikawa, K., Nakamura, S., Fukui, T., 2014. Biosynthesis of polyhydroxyalkanoate copolymers from methanol by Methylobacterium extorquens AM1 and the engineered strains under cobalt-deficient conditions. Appl. Microbiol. Biotechnol. 98, 3715–25. doi:10.1007/s00253-013-5490-9

Otting, G., Qian, Y.Q., Billeter, M., Muller1, M., Affolter ', M., Gehring1, W.J., Wuthrich, K., Wuthrich, K., 1990. Protein DNA contacts in the structure of a homeodomain -DNA complex determined by nuclear magnetic resonance spectroscopy in solution. EMBO J. 9, 3085–3092.

Pédelacq, J.-D., Cabantous, S., Tran, T., Terwilliger, T.C., Waldo, G.S., 2006. Engineering and characterization of a superfolder green fluorescent protein. Nat. Biotechnol. 24, 79–88. doi:10.1038/nbt1172

Peel D, Q.J., 1961. Microbial growth on C1 compounds. 1. Isolation and characterization of Pseudomonas AM1. Biochem J 81, 465–469.

Peyraud, R., Schneider, K., Kiefer, P., Massou, S., Vorholt, J. a, Portais, J.-C., 2011. Genome-scale reconstruction and system level investigation of the metabolic

network of Methylobacterium extorquens AM1. BMC Syst. Biol. 5, 189. doi:10.1186/1752-0509-5-189

Pietrocola, F., Galluzzi, L., Bravo-San Pedro, J.M., Madeo, F., Kroemer, G., 2015. Acetyl coenzyme A: A central metabolite and second messenger. Cell Metab. 21, 805–821. doi:10.1016/j.cmet.2015.05.014

Raman, S., Rogers, J.K., Taylor, N.D., Church, G.M., 2014. Evolution-guided optimization of biosynthetic pathways. Proc. Natl. Acad. Sci. 111, 17803–17808. doi:10.1073/pnas.1409523111

Sambrook, J., Russell, D.W., 2001. Molecular cloning: a laboratory manual. Cold Spring Harb.

Santos, C.N.S., Xiao, W., Stephanopoulos, G., 2012. Rational, combinatorial, and genomic approaches for engineering L-tyrosine production in Escherichia coli. Proc. Natl. Acad. Sci. 109, 13538–13543. doi:10.1073/pnas.1206346109/-/DCSupplemental.www.pnas.org/cgi/doi/10.1073/pnas.1206346109

Saridakis, V., Shahinas, D., Xu, X., Christendat, D., 2008. Structural Insight on the Mechanism of Regulation of the MarR Family of Proteins: High-Resolution Crystal Structure of a Transcriptional Repressor from Methanobacterium thermoautotrophicum. J. Mol. Biol. 377, 655–667. doi:10.1016/j.jmb.2008.01.001

Schrader, J., Schilling, M., Holtmann, D., Sell, D., Filho, M.V., Marx, A., Vorholt, J. a, 2009. Methanol-based industrial biotechnology: current status and future

perspectives of methylotrophic bacteria. Trends Biotechnol. 27, 107–15. doi:10.1016/j.tibtech.2008.10.009

Senior, P.J., Windass, J., 1980. The ICI single cell protein process. Biotechnol. Lett. 2, 205–210. doi:10.1007/BF01209434

Shen, P.-H., Wu, B., 2007. Over-expression of a hydroxypyruvate reductase in Methylobacterium sp. MB200 enhances glyoxylate accumulation. J. Ind. Microbiol. Biotechnol. 34, 657–63. doi:10.1007/s10295-007-0238-0

Sirirote P, Yamane T, S.S., 1986. Production of L-serine from methanol and glycine by resting cells of a methylotroph under automatically controlled conditions. J Ferment Technol 64, 389–396.

Sonntag, F., Kroner, C., Lubuta, P., Peyraud, R., Horst, A., Buchhaupt, M., Schrader, J., 2015. Engineering Methylobacterium extorquens for de novo synthesis of the sesquiterpenoid α-humulene from methanol. Metab. Eng. 32, 82–94. doi:10.1016/j.ymben.2015.09.004

Spiro, S., 1994. The FNR family of transcriptional regulators. Antonie Van Leeuwenhoek 66, 23–36.

Tan, F., Wu, B., Dai, L., Qin, H., Shui, Z., Wang, J., Zhu, Q., Hu, G., 2016. Using global transcription machinery engineering ( gTME ) to improve ethanol tolerance of Zymomonas mobilis. Microb. Cell Fact. 15, 1–9. doi:10.1186/s12934-015-0398-y

Tang, S.-Y., Cirino, P.C., 2011. Design and Application of a Mevalonate-Responsive Regulatory Protein. Angew. Chemie 123, 1116–1118. doi:10.1002/ange.201006083

Vuilleumier, S., Chistoserdova, L., Lee, M.-C., Bringel, F., Lajus, A., Zhou, Y., Gourion, B., Barbe, V., Chang, J., Cruveiller, S., Dossat, C., Gillett, W., Gruffaz, C., Haugen, E., Hourcade, E., Levy, R., Mangenot, S., Muller, E., Nadalig, T., Pagni, M., Penny, C., Peyraud, R., Robinson, D.G., Roche, D., Rouy, Z., Saenampechek, C., Salvignol, G., Vallenet, D., Wu, Z., Marx, C.J., Vorholt, J. a, Olson, M. V, Kaul, R., Weissenbach, J., Médigue, C., Lidstrom, M.E., 2009. Methylobacterium genome sequences: a reference blueprint to investigate microbial metabolism of C1 compounds from natural and industrial sources. PLoS One 4, e5584. doi:10.1371/journal.pone.0005584

Xu, P., Wang, W., Li, L., Bhan, N., Zhang, F., Koffas, M.A.G., 2014. Design and kinetic analysis of a hybrid promoter-regulator system for malonyl-CoA sensing in Escherichia coli. ACS Chem. Biol. 9, 451–458. doi:10.1021/cb400623m

Yang, J., Yan, R., Roy, A., Xu, D., J, P., Zhang, Y., 2015. The I-TASSER Suite: Protein structure and function prediction. Nat. Methods 12, 7–8. doi:10.1038/nmeth.3213

Yang, S., Matsen, J.B., Konopka, M., Green-Saxena, A., Clubb, J., Sadilek, M., Orphan, V.J., Beck, D., Kalyuzhnaya, M.G., 2013. Global Molecular Analyses of Methane Metabolism in Methanotrophic Alphaproteobacterium, Methylosinus

trichosporium OB3b. Part II. Metabolomics and 13C-Labeling Study. Front. Microbiol. 4, 70. doi:10.3389/fmicb.2013.00070

Zhang, X., Reeder, T., Schleif, R., 1996. Transcription activation parameters at ara pBAD. J. Mol. Biol. 258, 14–24. doi:10.1006/jmbi.1996.0230

Zhu, W.-L., Cui, J.-Y., Cui, L.-Y., Liang, W.-F., Yang, S., Zhang, C., Xing, X.-H., 2016. Bioconversion of methanol to value-added mevalonate by engineered Methylobacterium extorquens AM1 containing an optimized mevalonate pathway. Appl. Microbiol. Biotechnol. 100, 2171–2182. doi:10.1007/s00253-015-7078-z

Zhuo, Y., Zhang, W., Chen, D., Gao, H., Tao, J., Liu, M., Gou, Z., Zhou, X., Ye, B., Zhang, Q., Zhang, S., Zhang, L., 2010. Reverse biological engineering of to enhance the production of avermectins in an industrial strain of Streptomyces avermitilis. Proc. Natl. Acad. Sci. 107, 11250–11254. doi:10.1073/pnas.1006085107/-/DCSupplemental.www.pnas.org/cgi/doi/10.1073/pnas.1006085107

Figures and tables

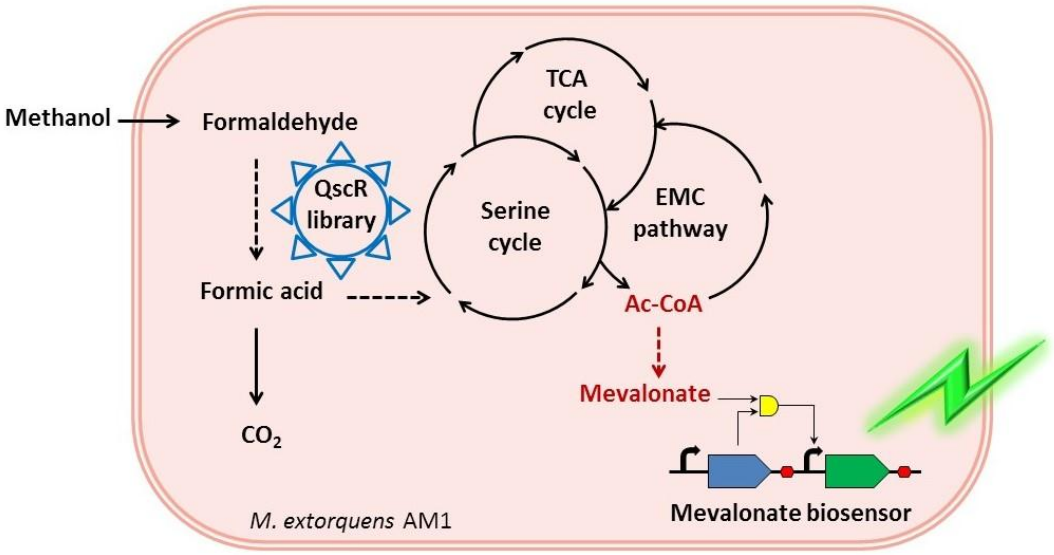


Fig. 1. Sensor-assisted transcriptional regulator engineering (SATRE) approach in M. extorquens AM1. QscR is the regulator of the serine cycle and thus the mutations in QscR created by error-prone PCR and the QscR library introduced in the host cells could shift the carbon flux toward acetyl-CoA (Ac-CoA) accumulation. A heterologous mevalonate synthesis pathway was introduced to transform acetyl-CoA into mevalonate along with a mevalonate biosensor that transforms intracellular mevalonate concentration into GFP fluorescence (as indicated by the green lightning bolt; see Fig. 2 for more details about the biosensor). The resultant strain was used for high-throughput screening for the high mevalonate production strains by FACS. TCA, tricarboxylic acid; EMC, ethylmalonyl-CoA; Ac-CoA, acetyl-CoA;

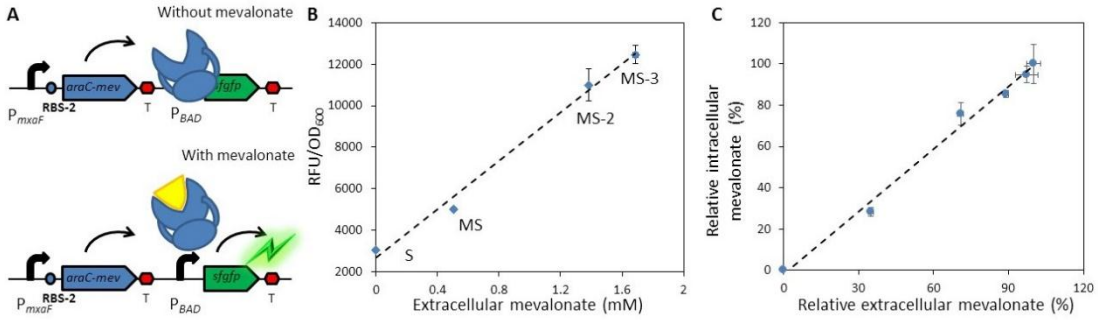


Fig. 2. Scheme and performance analysis of the mevalonate biosensor engineered for M. extorquens AM1. (A) The mevalonate biosensor is based on the arabinose operon. The original regulatory protein of AraC was replaced with AraC-mev (T24L, H80L, Y82L, H93R), which responds to mevalonate under the transcription of the $P_{mxaF}$ promoter. The regulatory protein AraC-mev blocks transcription from the $P_{BAD}$ promoter in the absence of mevalonate. In contrast, a mixture of AraC-mev and mevalonate binds to the $P_{BAD}$ promoter and activates the transcription combined with RNA polymerase (RNA polymerase not shown), leading to sfgfp transcription and, ultimately, GFP production, so that this sensor can be induced by mevalonate and the intracellular mevalonate concentration can be detected by the fluorescent signal. Black curved arrows represent the promoters; blue circles represent the RBS of araC-mev; blue pentagons represent genes; red hexagons represent terminators (T); blue protein represents Arac-mev regulatory protein; yellow wedge represents mevalonate; green lightning shape represents green fluorescent protein (GFP); (B) Response curve of the mevalonate biosensor in the strains S, MS, MS-2 and MS-3, showing a good linear relationship within 0-1.7 mM extracellular mevalonate concentration. The relative fluorescence intensity was normalized to the $OD_{600}$. (C) Relationship between intracellular and extracellular mevalonate concentrations in strain MS. The extracellular and intracellular mevalonate concentrations were determined by a gas chromatography. Data are shown as the mean ± SD, n = 3.

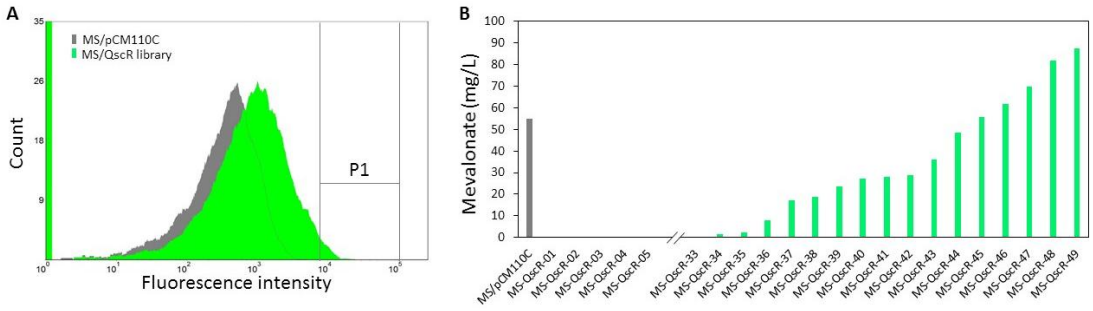


Fig. 3. FACS screening for the MS/pQscR library strain. (A) FACS analysis of the MS/pQscR library strain. Results are shown for both the control strain MS/pCM110C and for MS/pQscR library strain. Cells with the highest fluorescence (in area P1, uppermost 2% of cells) were sorted for single-cell culture. (B) Mevalonate titer by single-cell culture among the screened library. Forty-nine individually cultured cells were analyzed, along with a culture of MS/pCM110C cells as control. Strains MS-QscR-06 to MS-QscR-32 also showed no measurable mevalonate production (data not shown). The extracellular mevalonate concentration was determined after 5 d culture.

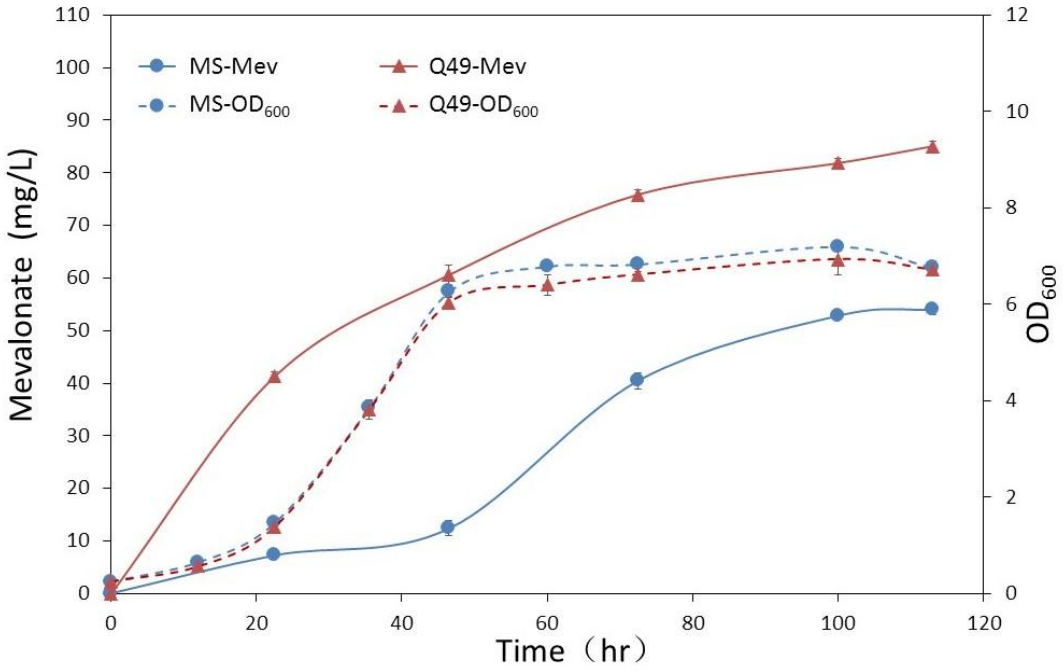


Fig. 4. Shake flask culture of strains MS/pCM110C and Q49. Solid lines represent the extracellular mevalonate concentration, as determined by a gas chromatography, and dashed lines represent the growth curve. Data are shown as the mean ± SD, n = 3.

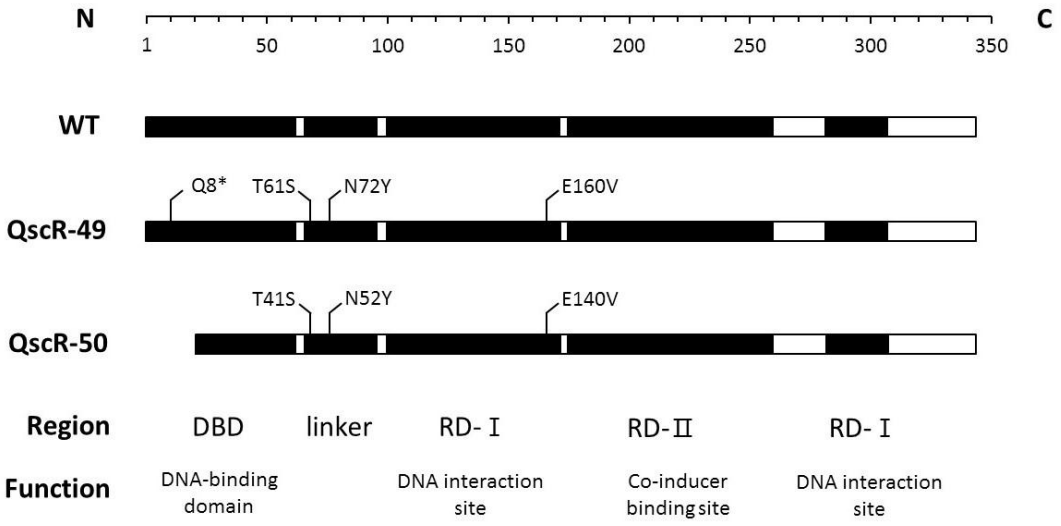


Fig. 5. Sequence analysis of QscR-49. Sequence analysis of QscR-49 resulted in the characterization of four amino acid changes in Q49 as shown here. QscR-50 was the generated from QscR-49, amplified from the second start codon. Conserved regions and their proposed functions are exhibited. WT, wild type; DBD, DNA-binding domain.

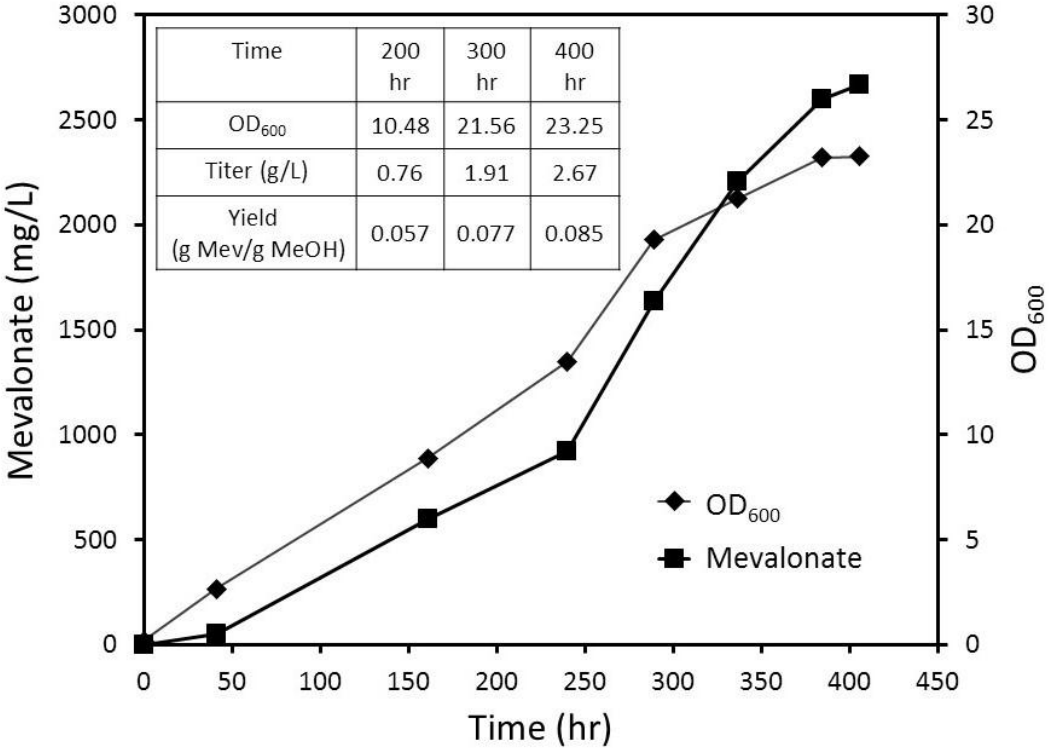


Fig. 6. Fed-batch fermentation of strain Q49 in a 5-L bioreactor. Mev, mevalonate; MeOH, methanol;

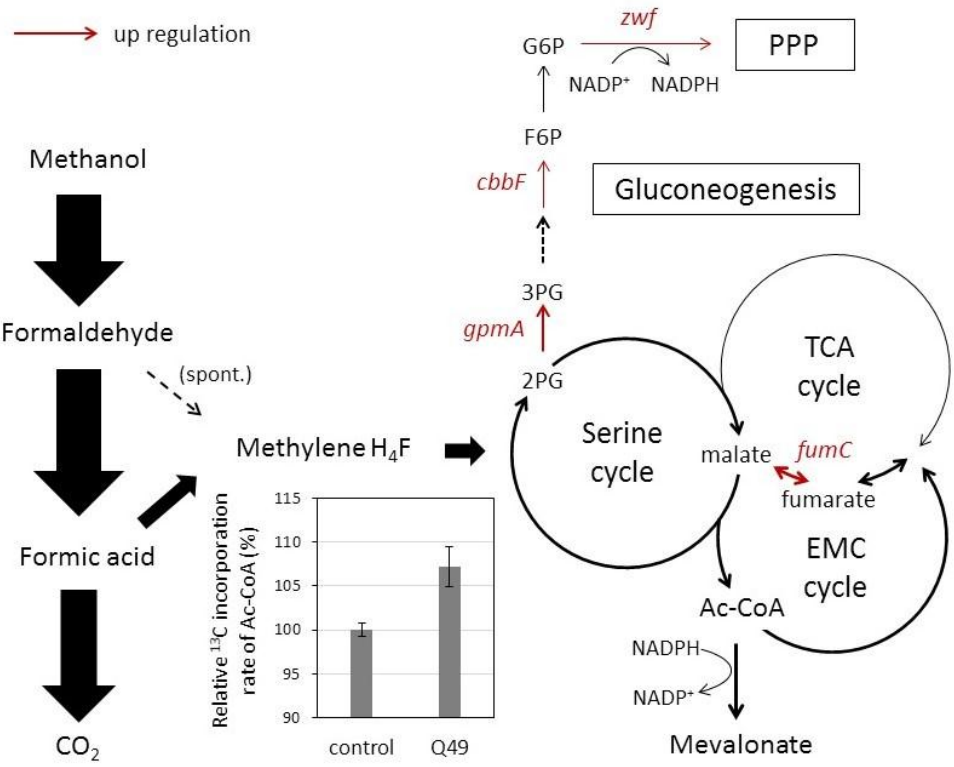


Fig. 7. Acetyl-CoA flux analysis and transcriptional analysis of strain Q49. $^{13}C$ labeling analysis revealed that acetyl-CoA flux of Q49 was 7% higher than that of control strain MS/pCM110C. Transcriptional analysis revealed that two genes in gluconeogenesis and one key gene in the pentose phosphate pathway were up-regulated. In addition, fumC, the gene product of which functions in both the TCA cycle and EMC cycle was also up-regulated. Other central metabolic pathways did not change. Arrow size represents the relative carbon flux. TCA, tricarboxylic acid cycle; EMC, ethylmalonyl-CoA cycle; PPP, pentose phosphate pathway; 2PG, 2-phosphoglycerate; 3PG, 3-phosphoglycerate; F6P, fructose-6-phosphate; G6P, glucose-6-phosphate; Ac-CoA, acetyl-CoA; gpmA, the gene encoding phosphoglyceromutase; cbbF, the gene encoding fructose-1,6-bisphosphatase; zwf, the gene encoding glucose-6-phosphate-1-dehydrogenase; fumC, the gene encoding fumarase C.

Table 1

Strains and plasmids used in this work.

| Strain or plasmid | Characteristics | Source |
|---|---|---|
| Strains | | |
| M. extorquens AM1 | Wild-type strain | NCIMB (NCIMB9133) |
| E. coli DH5α | Wild-type strain | Biomed |
| AM1 | M. extorquens AM1ΔcelABC | This work |
| S | AM1ΔcelABC::Sensor-4 | This work |
| MS | SΔ attTn7::Mvt-3, $km^R$ | This work |
| MS-2 | S/pMVT, $Km^R$ | This work |
| MS-3 | MS/pARBSU1, $km^R$, $Tet^R$ | This work |
| AM1Δqscr | AM1Δqscr | This work |
| AM1-qscr | AM1/pCM110-qscr | This work |
| AM1-ftfl | AM1/pCM110-ftfl | This work |
| Plasmids | | |
| pCM110 | M. extorquens AM1 expression vector ($P_{mxaF}$,$Tet^R$) | (C. J. Marx and Lidstrom, 2001) |
| pCM110A | Derived from pCM110, tetracycline resistance gene was replaced with ampicillin resistance gene, $Amp^R$ | This work |
| pCM110C | Derived from pCM110, tetracycline resistance gene was replaced with chloramphenicol resistance gene, $Cm^R$ | This work |

| | | |
|---|---|---|
| pCM110-qscr | pCM110A ($P_{mxaF}$::RBS of $P_{alkB}$::qscr::terminator), $Amp^R$ | This work |
| pCM110-ftfl | pCM110A ($P_{mxaF}$::RBS of $P_{alkB}$::ftfl::terminator), $Amp^R$ | This work |
| pSensor-1 | mevalonate biosensor-1, pCM110A (terminator::arac-mev::$P_c$::$P_{BAD}$::RBS of $P_{alkB}$::sfgfp::terminator), $Cm^R$ | This work |
| pSensor-2 | mevalonate biosensor-2, pCM110A ($P_{mxaF}$::RBS of $P_{alkB}$::arac-mev::terminator::$P_{BAD}$::RBS of $P_{alkB}$::sfgfp::terminator), $Cm^R$ | This work |
| pSensor-3 | mevalonate biosensor-3, pCM110A ($P_{mxaF}$::RBS of $P_{mxaF}$::arac-mev::terminator::$P_{BAD}$::RBS of $P_{alkB}$::sfgfp::terminator), $Cm^R$ | This work |
| pSensor-4 | mevalonate biosensor-4, pCM110A ($P_{mxaF}$:: RBS of $P_{mxaF}$::arac-mev::terminator::$P_{BAD}$::sfgfp::terminator), $Cm^R$ | This work |
| pQscR library | pCM110C ($P_{qscr}$::qscr library::terminator), $Cm^R$ | This work |
| pQ49 | a single mutant isolated from the pQscR library with four mutations (Q8*, T61S, N72Y, E160V), $Cm^R$ | This work |
| pQ50 | N-terminally truncated QscR-49 protein (T41S, N52Y, E140V), $Cm^R$ | This work |
| pK18mobsacB | Plasmid used for homologous recombination | (Kvitko and Collmer, 2011) |
| pT18 | Derived from pK18mobsacB, the nptII resistance gene was replaced with tetracycline resistance gene, $Tet^R$ | This work |

| | | |
|---|---|---|
| pT18-qscr | pT18 with upstream and downstream fragments of qscr (~1000 bp each), $Tet^R$ | This work |
| pT18-Sensor-4 | pT18 with upstream and downstream fragments of celABC cluster (~1000 bp each) and Sensor-4 fragment was inserted between upstream and downstream fragments, $Tet^R$ | This work |
| pARBSU1 | Plasmid containing the mevalonate synthesis pathway | (Zhu et al., 2016) |
| pMvt-3 | Mevalonate synthesis pathway optimized from pARBSU1 with RBS engineering of HMGR | This work |
| pT18-Mvt-3 | pT18 with upstream and downstream fragments of attTn7 site (~1000 bp each), the Mvt-3 fragment was inserted between the upstream and downstream fragments, $Tet^R$, $km^R$ | This work |



Highlights：

1. First construction of a mevalonate biosensor and establishment of high through-put screening method for Methylobacterium extorquens AM1.
2. First sensor-assisted transcriptional regulator engineering (SATRE) to control carbon flux in Methylobacterium extorquens AM1.
3. Up to 0.055 mol acetyl-CoA / mol methanol in fed-batch fermentation.